Extracellular Fluid Flow Induces Shallow Quiescence Through Physical and Biochemical Cues

Bi Liu [1,2†], Xia Wang [2,3†], Linan Jiang [4*], Jianhua Xu [1], Yitshak Zohar [4] and Guang Yao [2*]

[1]School of Pharmacy, Fujian Provincial Key Laboratory of Natural Medicine Pharmacology, Fujian Medical University, Fuzhou, China, [2]Department of Molecular and Cellular Biology, University of Arizona, Tucson, AZ, United States, [3]College of Animal Science and Technology, Northwest A&F University, Yangling, China, [4]Aerospace and Mechanical Engineering, University of Arizona, Tucson, AZ, United States

The balance between cell quiescence and proliferation is fundamental to tissue physiology and homeostasis. Recent studies have shown that quiescence is not a passive and homogeneous state but actively maintained and heterogeneous. These cellular characteristics associated with quiescence were observed primarily in cultured cells under a static medium. However, cells *in vivo* face different microenvironmental conditions, particularly, under interstitial fluid flows distributed through extracellular matrices. Interstitial fluid flow exerts shear stress on cells and matrix strain, and results in continuous replacement of extracellular factors. In this study, we analyzed individual cells under varying fluid flow rates in microfluidic devices. We found quiescence characteristics previously identified under conventional static medium, including serum signal-dependant quiescence entry and exit and time-dependant quiescence deepening, are also present under continuous fluid flow. Furthermore, increasing the flow rate drives cells to shallower quiescence and become more likely to reenter the cell cycle upon growth stimulation. This effect is due to flow-induced physical and biochemical cues. Specifically, increasing shear stress or extracellular factor replacement individually, without altering other parameters, results in shallow quiescence. We show our experimental results can be quantitatively explained by a mathematical model connecting extracellular fluid flow to an Rb-E2f bistable switch that regulates the quiescence-to-proliferation transition. Our findings uncover a previously unappreciated mechanism that likely underlies the heterogeneous responses of quiescent cells for tissue repair and regeneration in different physiological tissue microenvironments.

Keywords: cellular quiescence, quiescence depth, extracellular fluid flow, flow shear stress, extracellular factors, microenvironment, microfluidics, mathematical model

INTRODUCTION

Quiescence is a dormant, non-proliferative cellular state. Quiescent cells, however, still maintain the potential to proliferate upon physiological signals, making them distinct from other dormant cells that are irreversibly arrested, such as those in senescence or terminal differentiation. Activating quiescent cells (e.g., adult stem and progenitor cells) to proliferate is fundamental to tissue homeostasis and repair (Coller et al., 2006; Wilson et al., 2008; Li and Clevers, 2010; Cheung and Rando, 2013). Quiescence has long been viewed as a passive cellular state lacking cell cycle

activity. Recent studies, however, have revealed that quiescence is rather actively maintained and highly heterogeneous (Coller et al., 2006; Sang et al., 2008; Cheung and Rando, 2013; Spencer et al., 2013; Wang et al., 2017).

The heterogeneity of quiescent cells in their proliferation potential can be described as a graded depth. Cells in deeper quiescence require stronger growth stimulation and take longer to exit quiescence and reenter the cell cycle than in shallower quiescence (Augenlicht and Baserga, 1974; Kwon et al., 2017; Fujimaki et al., 2019). Hepatocytes in older rats are an example of deeper quiescent cells, displaying a longer delay before reentering the cell cycle and reinitiating DNA replication following partial hepatectomy, as compared to those in younger rats (Bucher, 1963). Certain muscle and neural stem cells after tissue injury are examples of shallow quiescent cells, primed to reenter the cell cycle faster upon the next damage (Rodgers et al., 2014; Llorens-Bobadilla et al., 2015). The dysregulation of cellular quiescence depth can lead to disrupted tissue homeostasis, exhibiting either an insufficient number of growing cells due to an abnormally deep quiescence, or a depleted pool of quiescent stem and progenitor cells due to an abnormally shallow quiescence (Orford and Scadden, 2008; Cheung and Rando, 2013; Fujimaki and Yao, 2020).

Although dormant and non-proliferative, quiescent cells reside in and interact with dynamic microenvironments. A particular microenvironmental factor is the interstitial fluid flowing over tissue cells, which transports nutrients and other dissolved molecules that influence cellular activities (Jain, 1987; Swartz and Fleury, 2007; Freund et al., 2012; Yao et al., 2013). Interstitial flow also generates mechanical shear stress on cells, which affects cell morphology, migration, growth, and differentiation (Jain, 1987; Ng and Swartz, 2003; Tarbell et al., 2005; Swartz and Fleury, 2007; Polacheck et al., 2011; Shirure et al., 2017; Chen et al., 2019). To date, though, cellular quiescence has been mostly studied in cell cultures under static medium or in animal models without examining the effects of interstitial fluid flow. Whether and how extracellular fluid flow affects cellular quiescence remain largely unknown.

In this study, we examined the effects of extracellular fluid flow on cellular quiescence depth using a microfluidic system with a controllable medium flow rate. First, we found many quiescence characteristics previously observed in cell cultures under a static medium were also present in the microfluidic system under continuous medium flow. Furthermore, the medium flow affected cellular quiescence depth, and thus, the likelihood of cell cycle reentry upon growth stimulation. This result was further explained by the combined effect of flow-induced hydrodynamic shear stress and extracellular substance replacement. Lastly, the experimental results were integrated into a mathematic model that helps understand and predict how extracellular fluid flow modulates quiescence depth. To the best of our knowledge, this study is the first to characterize the effects of extracellular fluid flow on cellular quiescence, which could help better understand the heterogeneous response of quiescent cells for tissue repair and regeneration in different physiological contexts of living tissues.

MATERIAL AND METHODS

Microfluidic Device Design and Fabrication

A microfluidic system was developed to study cellular quiescence under medium flow. To obtain sufficient numbers of cells for flow cytometry analyses, a microfluidic device was designed featuring a straight channel 420 μm in height, 4 mm in width, and 4 cm in length. The microdevices, made of optically transparent polydimethylsiloxane (PDMS, Sylgard 184, *Dow Corning* Corporation, 3097358-1004), also allow real-time imaging of cells during experimentation.

The device fabrication process, illustrated in **Figure 1**, started with the fabrication of a master mold. The mold with features of microchannel patterns was made in an aluminum block using a computer numerical control (CNC) machine based on a 3D Computer-Aided Design (CAD). PDMS mixture, consisting of 10:1 base and curing agent, was poured onto the mold. After air bubble removal from the mixture under vacuum, the PDMS was cured at 55°C for 3 h. The cured PDMS substrate was then peeled off the mold with formed microchannel grooves (**Figure 1A**). After punching inlet and outlet holes at the two ends of a channel, the PDMS microchannel was bonded with a glass slide following oxygen plasma treatment of the bonding surfaces (**Figure 1B**). Next, a pair of inlet and outlet tubing adapters was assembled for each device to connect the microchannel to the external flow control system. The device fabrication and packaging were completed with incubation at 55°C for an hour to enhance the bonding strength (**Figure 1C**). Prior to experiments, the microfluidic devices were sterilized by flowing ethanol through the microchannels, followed by UV irradiation for 1 h inside a biosafety hood. The inner surfaces of the microchannel were coated with 2% (w/w) fibronectin to enhance the adhesion of cells to the bottom surface.

Flow Rate and Flow-Induced Shear Stress

The total volume of medium in a microdevice (including tubing at the inlet/outlet of the channel but not connectors, **Figure 1C**) is approximately 140 μl, and the medium volume in the microfluidic channel alone is about 67 μl. In this study, a continuous medium flow with a fixed flow rate (5 or 20 μl/h) was fed into the channel to mimic the typical interstitial flow velocity in soft tissues (Swartz and Fleury, 2007) unless otherwise noted. Correspondingly, the flow rate, rather than the priming volume, is used to characterize the flow effect. We also consider the concentration of the bulk fluid is uniform spatially, and local diffusion and convection at the interfaces between the fluid and cells can be neglected.

Pressure-driven flow in a microchannel presents a non-uniform velocity profile, which gives rise to shear stress. The shear stress for a Newtonian fluid is directly proportional to the product of the velocity gradient and fluid viscosity. Assuming a 2-D parabolic velocity profile in a microchannel with a rectangular
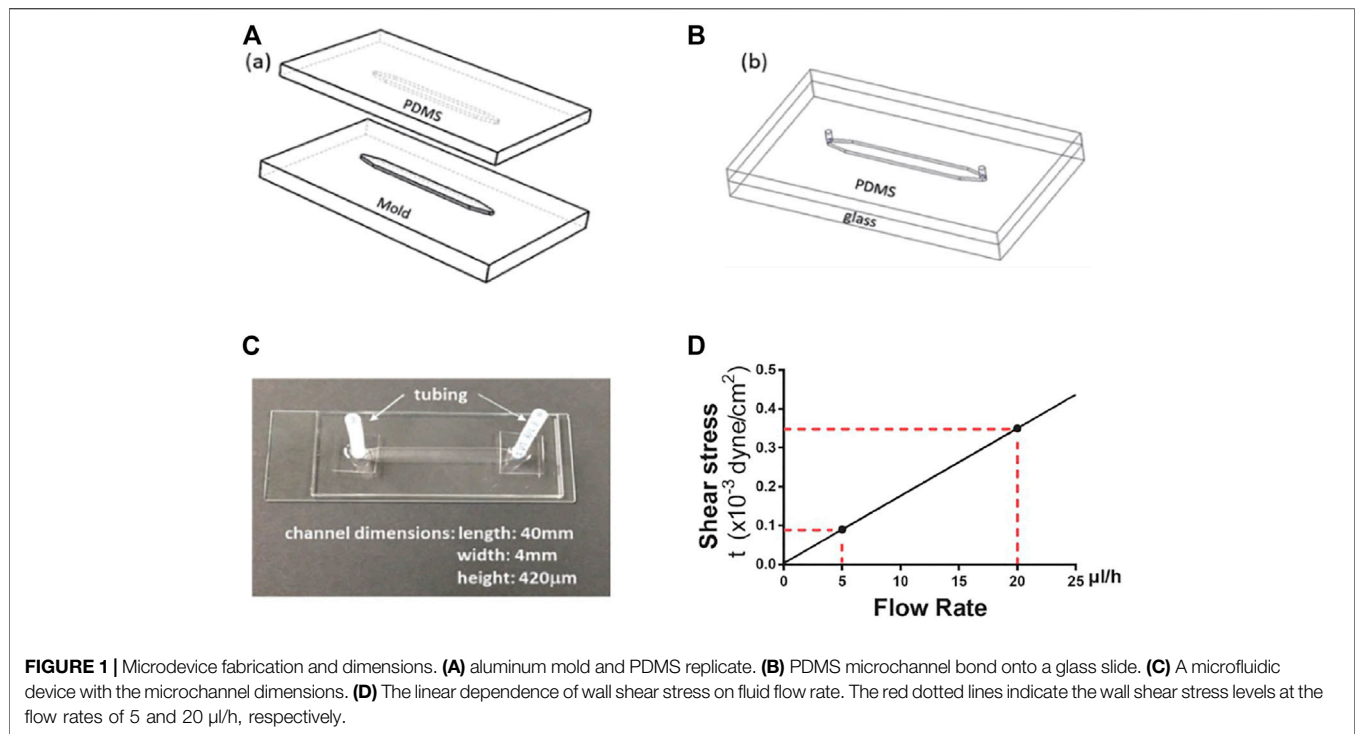
FIGURE 1 | Microdevice fabrication and dimensions. **(A)** aluminum mold and PDMS replicate. **(B)** PDMS microchannel bond onto a glass slide. **(C)** A microfluidic device with the microchannel dimensions. **(D)** The linear dependence of wall shear stress on fluid flow rate. The red dotted lines indicate the wall shear stress levels at the flow rates of 5 and 20 μl/h, respectively.

TABLE 1 | Flow-induced shear stress in medium containing varying dextran concentrations.

Dextran concentration (mg/ml)	Viscosity (cP)	Wall shear stress at 5 ul/h flow rate (10^{-3} dyne/cm^2)	Wall shear stress at 20 ul/h flow rate (10^{-3} dyne/cm^2)
0	0.73	0.09	0.35
25	1.95	0.23	0.93
50	4.64	0.55	2.20
100	23.78	2.82	11.28

cross-section, the wall shear stress, τ_w, experienced by cells attached on the bottom surface of the microchannel, is given by:

$$\tau_w = \frac{6\mu Q}{WH^2} \qquad (1)$$

where W and H are the microchannel width and height, respectively, μ is the fluid viscosity, and Q is the volumetric flow rate. For a fixed medium viscosity, estimated to be $\mu = 0.73$ cP at 37°C, and given the microchannel dimensions, $W = 4$ mm and $H = 420$ μm, the shear stress is linearly proportional to the fluid flow rate. Thus, the two flow rates used in this study, $Q = 5$ and 20 μl/h, correspond to shear stress values $\tau_w = 0.09 \times 10^{-3}$ and 0.35×10^{-3} dyne/cm^2, respectively (**Figure 1D**).

In **Eq. 1**, for a fixed flow rate and microchannel dimensions, wall shear stress is linearly proportional to the medium viscosity. Dextran (Sigma, D5251; ~ 500,000 average molecular weight) was dissolved in the medium in various final concentrations to obtain correspondingly various medium viscosities. **Table 1** summarizes the resultant dextran-containing medium concentrations,

viscosity at 37°C, and corresponding shear stress values for the two flow rates (Carrasco et al., 1989).

Cell Culture

REF/E23 cells used in this work were derived from rat embryonic fibroblasts REF52 cells as a single-cell clone containing a stably integrated E2f1 promoter-driven destabilized GFP reporter (E2f-GFP for short), as previously described (Yao et al., 2008). Cells were maintained at 37°C with 5% CO_2 in the growth medium: DMEM (Coning, 15013-CV supplemented with 2x Glutamax (Gibco, 35050)) containing 10% bovine growth serum BGS (HyClone, SH30541.03).

Quiescence Depth Measurement Under Extracellular Fluid Flow

To induce cellular quiescence, growing cells were trypsinized (Coning, 25052-CI), and 70 μl of cell suspension (0.6 million cells/ml) was seeded into a microfluidic channel; after cell

attachment on the bottom surface of the channel overnight, growth medium inside the channel was replaced by a continuous flow of serum-starvation medium (0.02% BGS in DMEM) at a designated flow rate controlled by a programmable syringe pump (Harvard PHD 2000). Cell morphologies were found comparable across the flow rate range (0–20 μl/h) (**Supplementary Figure S1A**). To induce quiescence exit, following serum starvation, the microdevice was disconnected from the flow-feeding setup (syringe and pump), and serum-stimulation medium (1–4% BGS in DMEM) was gently flowed into the micro-chamber using a pipette and a tip at the inlet tubing of the device. The medium change step is fast (<1 min for 140 μl medium) and identical to all quiescent cell groups, avoiding the bias in the exposure time of cells to the stimulation medium (if otherwise using slow flows at different flow rates, 5 or 20 μl/h). Cells were then incubated with serum-stimulation medium at static condition (again, identical to all quiescent cell groups). After 26 h of serum stimulation, cells inside the channel were harvested, and the intensities of E2f-GFP signals from individual cells were measured using a flow cytometer (BD LSR II). Flow cytometry data were analyzed using FlowJo software (version 10.0).

The percentage of cells with the E2f at the "On" state (E2f-On %) in a cell population after serum stimulation was used as an index for quiescence depth before stimulation: the smaller the E2f-On%, the deeper the quiescence depth prior to serum stimulation (Kwon et al., 2017). Consistent with our previous studies in static-medium experiments (Kwon et al., 2017; Wang et al., 2017; Fujimaki et al., 2019), E2f-On% was found comparable to the percentage of cells with EdU incorporation (EdU+%) in the microfluidic experiments under continuous flows (**Supplementary Figures S1B,C**). In the EdU incorporation assay, 1 μM EdU was added to the serum-stimulation medium at 0 h, and the EdU signal intensity was measured 30 h after serum stimulation by the Click-iT EdU assay following the manufacturer's protocol (ThermoFisher, C10634).

Mathematical Modeling and Stochastic Simulations

To account for the effects of extracellular fluid flow on quiescence depth, the fluid flow-associated terms were added to the serum response terms in our previously established Rb-E2F bistable switch model (**Supplementary Table S1**) (Yao et al., 2008). Based on the resultant ordinary differential equation (ODE) framework (**Supplementary Table S1**), a Langevin-type stochastic differential equation (SDE) model was constructed as follows (Gillespie, 2000; Lee et al., 2010):

$$X_i(t + \tau) = X_i(t) + \sum_{j=1}^{M} v_{ji} a_j [X(t)]\tau + \theta \sum_{j=1}^{M} v_{ji} \left(a_j [X(t)]\tau \right)^{1/2} \gamma$$
$$+ \delta\omega\tau^{1/2}$$

(2)

where the first two terms on the right account for deterministic kinetics, and the third and fourth terms represent intrinsic and

extrinsic noise, respectively. $X(t) = (X_1(t), \ldots, X_n(t))$ is the system state at time t. $X_i(t)$ is the molecule number of species i ($i = 1, \ldots, n$) at time t. The time evolution of the system is measured based on the rates $a_j[X(t)]$ ($j = 1, \ldots, M$) with the corresponding change of molecule number j described in v_{ji}. Factors γ and ω are two independent and uncorrelated Gaussian noises. Scaling factors θ and δ are implemented for the adjustment of intrinsic and extrinsic noise levels, respectively (unless otherwise noted, $\theta = 0.4$, $\delta = 40$, as selected to be consistent with the experimental data presented in **Figure 3**). Units of model parameters and species concentrations (**Supplementary Table S2**) in the ODE model were converted to molecule numbers. The E2f-On state was defined as the E2f molecule number at the 26th h after serum stimulation reaching beyond a threshold value of 300. All SDEs were implemented and solved in Matlab.

RESULTS

Quiescence Induction and Deepening Over Time are Consistent With or Without Medium Flow

To test whether and how extracellular fluid flow affects cellular quiescence, we cultured REF/E23 cells in microfluidic devices under medium flow (**Figure 1**). Two flow rates ($Q = 5$ and 20 μl/h) were used in this study; they generated average velocities of 0.82 and 3.33 μm/s on the microfluidic platform, respectively, which are on the order of typical interstitial flow velocity in soft tissues (Swartz and Fleury, 2007). Cells were seeded in microfluidic devices, and cell quiescence and proliferation status were assessed using a previously established and stably integrated E2f-GFP reporter (Yao et al., 2008), which was validated by standard EdU-incorporation assay in regular cell cultures (Kwon et al., 2017; Wang et al., 2017; Fujimaki et al., 2019) as well as here on the microfluidic platform (**Supplementary Figures S1B,C**; see Methods).

To induce quiescence, cells in microfluidic devices were cultured in serum-starvation medium (0.02% serum) for 4 days under a given extracellular fluid flow (5 or 20 μl/h). In these conditions, about 95% of cells or more entered quiescence (**Figures 2A,B**, 0.02% serum, 4-days), as indicated by the Off-state of the E2f-GFP reporter (E2f-Off for short, the lower/left mode of the E2f-GFP histograms in **Figure 2**). Quiescent cells were subsequently stimulated to reenter the cell cycle with serum at varying concentrations (without flow, see Methods for details). Cells were harvested after 26 h of serum stimulation, and the E2f-GFP reporter activity was measured by flow cytometry. With increasing serum conconcentrations (0.02–4% serum, 4 days, **Figure 2**), higher percentages of cells exited quiescence and reentered the cell cycle, as indicated by the On-state of the E2f-GFP reporter (E2f-On for short, the higher/right mode of the E2f-GFP histograms in **Figure 2**). The observations that cells entered quiescence upon serum deprivation under an extracellular fluid flow and then reentered the cell cycle upon
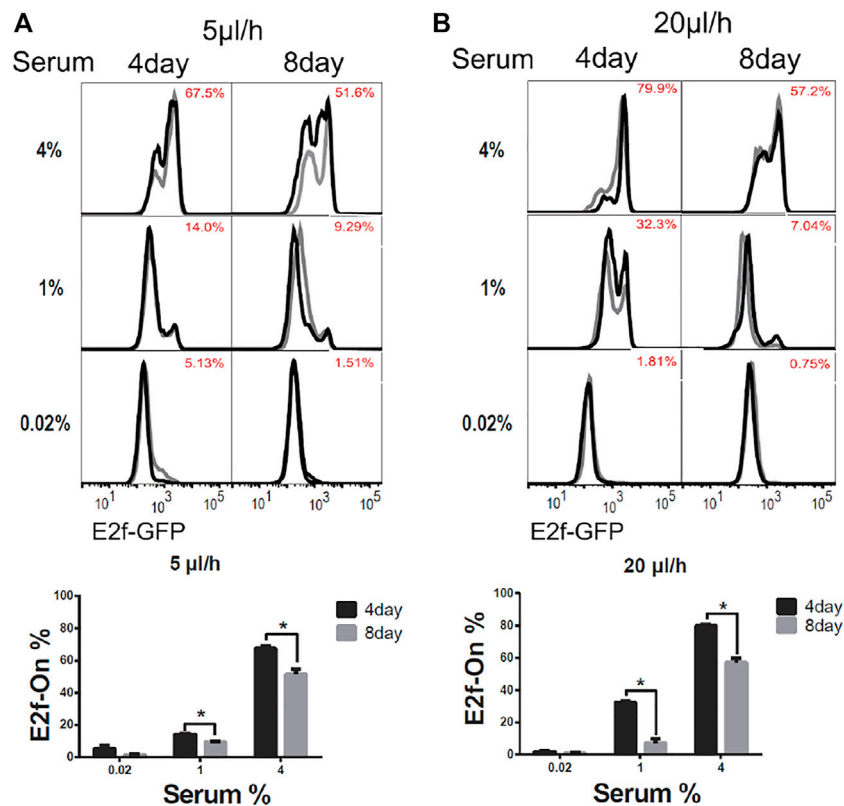
FIGURE 2 | Longer-term serum starvation under extracellular fluid flow leads to deeper quiescence. REF/E23 cells seeded in microfluidic devices were induced to and maintained in quiescence by culturing them in serum-starvation medium for either 4 or 8 days under the medium flow rates of 5 µl/h **(A)** and 20 µl/h **(B)**. Cells were subsequently stimulated with serum at the indicated concentrations for 26 h, and the E2f-On% were assayed. (Top) E2f-GFP histograms with red numbers indicating the average E2f-On% (the areas below the right "peaks" of the bimodal histograms; same below) from duplicate samples (black and grey). (Bottom) Statistic bar chart of the E2f-On% in cell populations (from the top) as a function of serum-starvation duration and serum concentration in serum-stimulation. Error bars, SEM ($n = 2$), $^*p < 0.05$.

serum stimulation are consistent with the cell behaviors in conventional static medium (Coller et al., 2006; Yao et al., 2008).

We next compared cells induced to quiescence by 8 *vs.* 4 days of serum starvation in the presence of extracellular fluid flow. Previous work, including ours, showed that cells moved into deeper quiescence when they remained quiescent for longer durations in conventional static-medium cell cultures (Augenlicht and Baserga, 1974; Owen et al., 1989; Kwon et al., 2017; Fujimaki et al., 2019). One may wonder, however, whether this phenotype was caused by the gradual depletion of nutrients in the static culture medium *in vitro,* which may behave differently *in vivo* under an interstitial fluid flow replenishing nutrients. In the microfluidic platform under a constant fluid flow (either 5 or 20 µl/h) during serum starvation, we found cells that remained quiescent for a longer period of time (8 days) entered a deeper quiescent state and became less likely to exit: they had a smaller E2f-On% upon a given serum stimulation than those that remained quiescent for a shorter time (4 days, **Figure 2**). Together, these results showed that cellular behaviors in 1) serum signal-dependant quiescence entry and exit and 2) quiescence deepening over time are consistent regardless

whether cells are in microfluidic devices exposed to extracellular fluid flows or in conventional static-medium cultures.

Fast Extracellular Fluid Flow Results in Shallow Quiescence

To examine whether and how extracellular fluid flow may affect cellular quiescence depth, we compared the cells induced to quiescence by serum starvation under different medium flow rates but otherwise in the same conditions. Specifically, cells in microfluidic devices were cultured in serum-starvation medium (0.02% serum) for 4 days under an extracellular fluid flow (0, 5, or 20 µl/h); serum-starvation medium was then replaced by serum-stimulation medium (1–4% serum) using a pipette—this medium change procedure in each microfluidic device was completed within 1 min (compared to otherwise more than 20 and 5 h under a pump-driven slow flow of 5 and 20 µl/h, respectively); cells were then cultured in static medium during serum stimulation. This identical serum-stimulation condition was applied in this study (see Methods for details), so that the subsequent cell cycle reenter
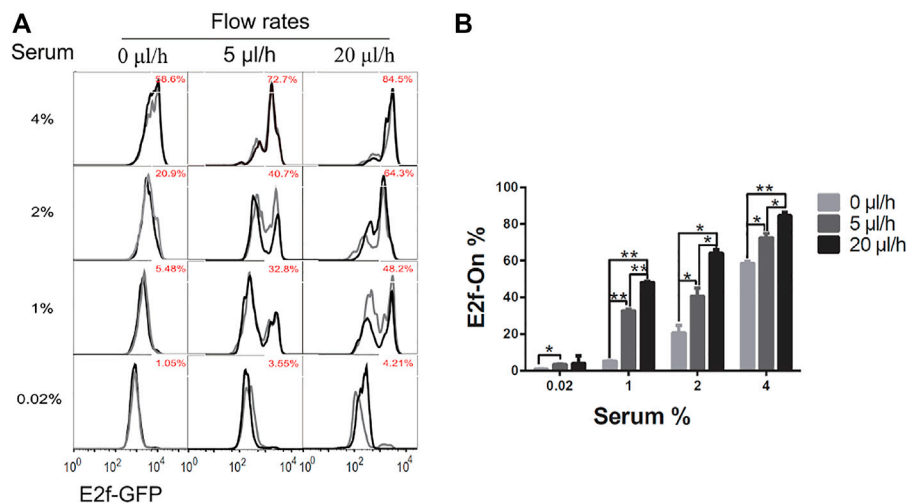
FIGURE 3 | Higher extracellular medium flow rates lead to shallower quiescence. REF/E23 cells seeded in microfluidic devices were induced to and maintained in quiescence by culturing them in serum-starvation medium for 4 days under various medium flow rates as indicated. Cells were then stimulated with serum at the indicated concentrations for 26 h, and the E2f-GFP signals were measured using flow cytometry. **(A)** The E2f-GFP histograms. Numbers in red indicate the average percentages of cells with E2f-GFP at the "On" state (see **Supplementary Figure S1D** for examples) based on duplicate samples (black and grey histograms). **(B)** Statistic bar chart of the E2f-On% in cell populations (from A) as a function of medium flow rate (in serum-starvation) and serum concentration (in serum-stimulation). Error bars, SEM (*n* = 2), *p < 0.05, **p < 0.01 (1-tailed t-test; the same below).

and thus the assessment of quiescence depth were not biased by different effective exposure time of cells to the serum-stimulation medium (if the medium was fed by different pump-driven flows) and thus comparable across different quiescent cell groups (which were induced by serum starvation under different medium flow rates).

Upon serum stimulation (with 1, 2, or 4% serum), the fraction of cells reentering the cell cycle from quiescence, as indicated by E2f-On% in **Figure 3**, were positively correlated with the medium flow rate applied to cells during quiescence induction (serum starvation). These results suggest that a higher extracellular fluid flow rate leads to shallower quiescence, from which cells are more likely to reenter the cell cycle upon stimulation.

Mechanical Shear Stress Drives Shallow Quiescence

Fluid flow introduces two types of cues to cells: 1) hydrodynamic shear stress (physical cue), and 2) continuous replenishment of nutrients and other compounds dissolved in the fluid and removal of local cell-secreted substances (collectively as extracellular factor replacement; biochemical cue). To determine whether these physical and biochemical cues act agonistically or antagonistically (thereby potentiating or attenuating the combined effect) in affecting cellular quiescence depth, we next conducted experiments to delineate the effect of each of the two cues.

To isolate the effect of mechanical shear stress from that of extracellular factor replacement on cellular quiescence depth, the viscosity of the culture medium was varied while its flow rate (and thus the pace of extracellular fluid replacement) was maintained at a constant level. The flow-induced shear stress is linearly

proportional to the viscosity of working fluid (**Eq. 1**), which can be manipulated by varying the amount of high-molecular-weight dextran dissolved in the medium (**Table 1**).

Accordingly, REF/E23 cells were first induced to quiescence by culturing them in the serum-starvation medium containing 0, 25, 50, or 100 mg/ml high molecular weight (~ 500,000) dextran, respectively, for 4 days under 5 or 20 µl/h flow rate. The cells were then stimulated with 2% or 4% serum for 26 h, and the fraction of cells that exited quiescence (E2f-On%) was measured. As shown in **Figures 4A,B**, E2f-On% increased with increasing dextran concentration in the serum-starvation medium under either 5 or 20 µl/h flow rate. By contrast, cells cultured in static serum-starvation medium containing the same higher dextran concentration entered deeper rather than shallower quiescence (**Supplementary Figure S2**; see Discussion). These results suggest that the dextran-induced shallow quiescence in the presence of extracellular fluid flow was primarily due to the viscosity-dependent shear stress (instead of other dextran-associated effects such as being a metabolic source). The higher dextran concentration, thus higher viscosity, of the medium flow generates higher shear stress under a continuous flow rate (5 or 20 µl/h, see **Table 1**; but not static 0 µl/h). Put together, our results showed that increasing only the fluid flow shear stress, while keeping the same flow rate and pace of extracellular factor replacement, leads to shallower quiescence.

Extracellular Factor Replacement Drives Shallow Quiescence

The effect of continuous extracellular factor replacement on cellular quiescence depth was examined next. Some of the extracellular factors (such as nutrients) are expected to
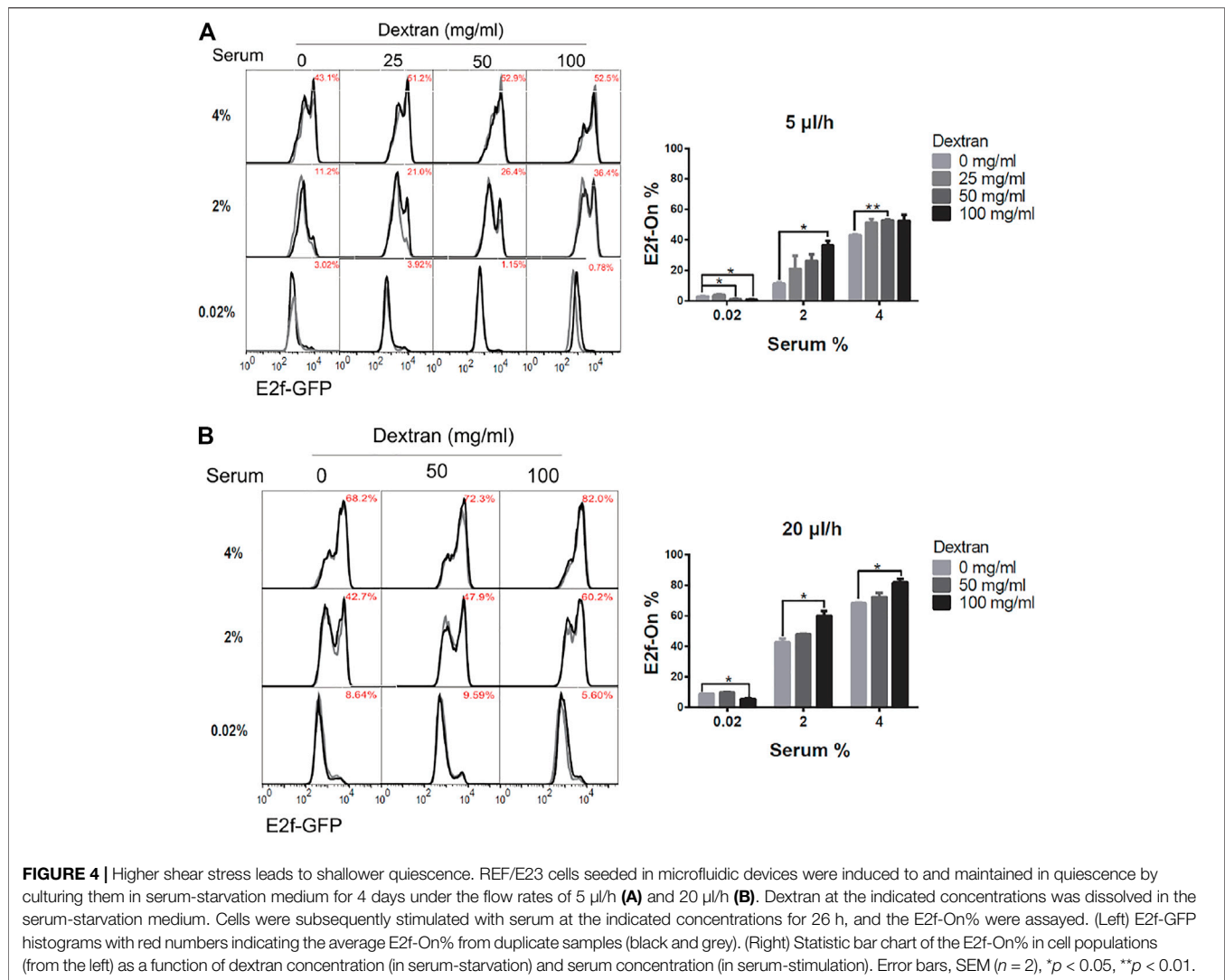
FIGURE 4 | Higher shear stress leads to shallower quiescence. REF/E23 cells seeded in microfluidic devices were induced to and maintained in quiescence by culturing them in serum-starvation medium for 4 days under the flow rates of 5 µl/h **(A)** and 20 µl/h **(B)**. Dextran at the indicated concentrations was dissolved in the serum-starvation medium. Cells were subsequently stimulated with serum at the indicated concentrations for 26 h, and the E2f-On% were assayed. (Left) E2f-GFP histograms with red numbers indicating the average E2f-On% from duplicate samples (black and grey). (Right) Statistic bar chart of the E2f-On% in cell populations (from the left) as a function of dextran concentration (in serum-starvation) and serum concentration (in serum-stimulation). Error bars, SEM ($n = 2$), *$p < 0.05$, **$p < 0.01$.
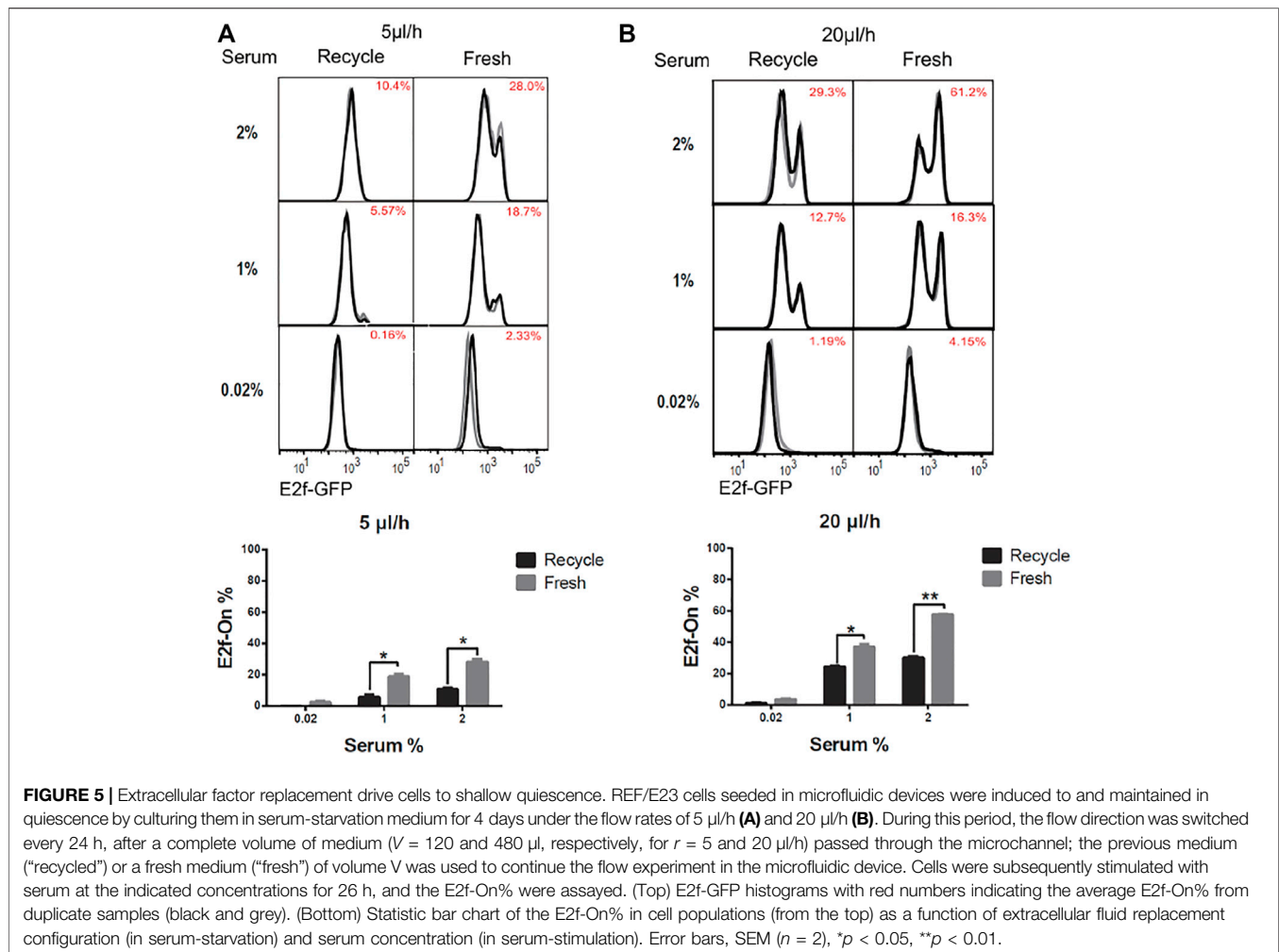
facilitate quiescence exit and cell cycle reentry, while others may play inhibitory roles (such as certain extracellular matrix (ECM) factors secreted by fibroblasts). To assess the net effect of extracellular factor replacement, while decoupling it from the effect of mechanical shear stress, we set up two test configurations. In the first "recycled-medium" configuration, a total fluid volume of either $V = 120$ or 480 µl oscillated back-and-forth through the microchannel at a constant flow rate of either $Q = 5$ or 20 µl/h, respectively. Thus, when the flow direction was switched every 24 h, the complete fluid volume V passed through the microchannel once. In the second "fresh-medium" configuration, the fluid oscillated exactly as in the first configuration, but fresh medium of volume V was supplied to replace previous medium at each flow direction switch. In both the recycled-medium and fresh-medium experiments, cells were serum-starved for 4 days at a given flow rate Q (5 or 20 µl/h) and subsequently stimulated with serum (1 and 2%, respectively) for 26 h.

The quiescence depth measurements are shown in **Figure 5**. The fractions of cells exiting quiescence and reentering cell cycle

(E2f-On%) were significantly higher in 'fresh-medium' than in "recycled-medium" at a given serum stimulation condition. These results were obtained at the same flow rate (either 5 or 20 µl/h) and thus under the same mechanical shear stress. The difference that the cells experienced was medium replacement: once per 24 h during the 4-days serum-starvation in the fresh-medium configuration, whereas no medium replacement during the same period in the recycled-medium configuration. These results suggest that with the flow rate and shear stress being equal, extracellular factor replacement alone (as in "fresh-medium") induces shallower quiescence than without such a replacement (as in "recycled-medium").

A Dynamic Model of Extracellular Fluid Flow Regulating Quiescence Depth

We next sought to develop a mathematical model to gain potential mechanistic insight into the effects of extracellular fluid flow on cellular quiescence depth. Previously, we have shown that the Rb-E2f pathway functions as a bistable gene-

FIGURE 5 | Extracellular factor replacement drive cells to shallow quiescence. REF/E23 cells seeded in microfluidic devices were induced to and maintained in quiescence by culturing them in serum-starvation medium for 4 days under the flow rates of 5 μl/h **(A)** and 20 μl/h **(B)**. During this period, the flow direction was switched every 24 h, after a complete volume of medium (V = 120 and 480 μl, respectively, for r = 5 and 20 μl/h) passed through the microchannel; the previous medium ("recycled") or a fresh medium ("fresh") of volume V was used to continue the flow experiment in the microfluidic device. Cells were subsequently stimulated with serum at the indicated concentrations for 26 h, and the E2f-On% were assayed. (Top) E2f-GFP histograms with red numbers indicating the average E2f-On% from duplicate samples (black and grey). (Bottom) Statistic bar chart of the E2f-On% in cell populations (from the top) as a function of extracellular fluid replacement configuration (in serum-starvation) and serum concentration (in serum-stimulation). Error bars, SEM (n = 2), *p < 0.05, **p < 0.01.
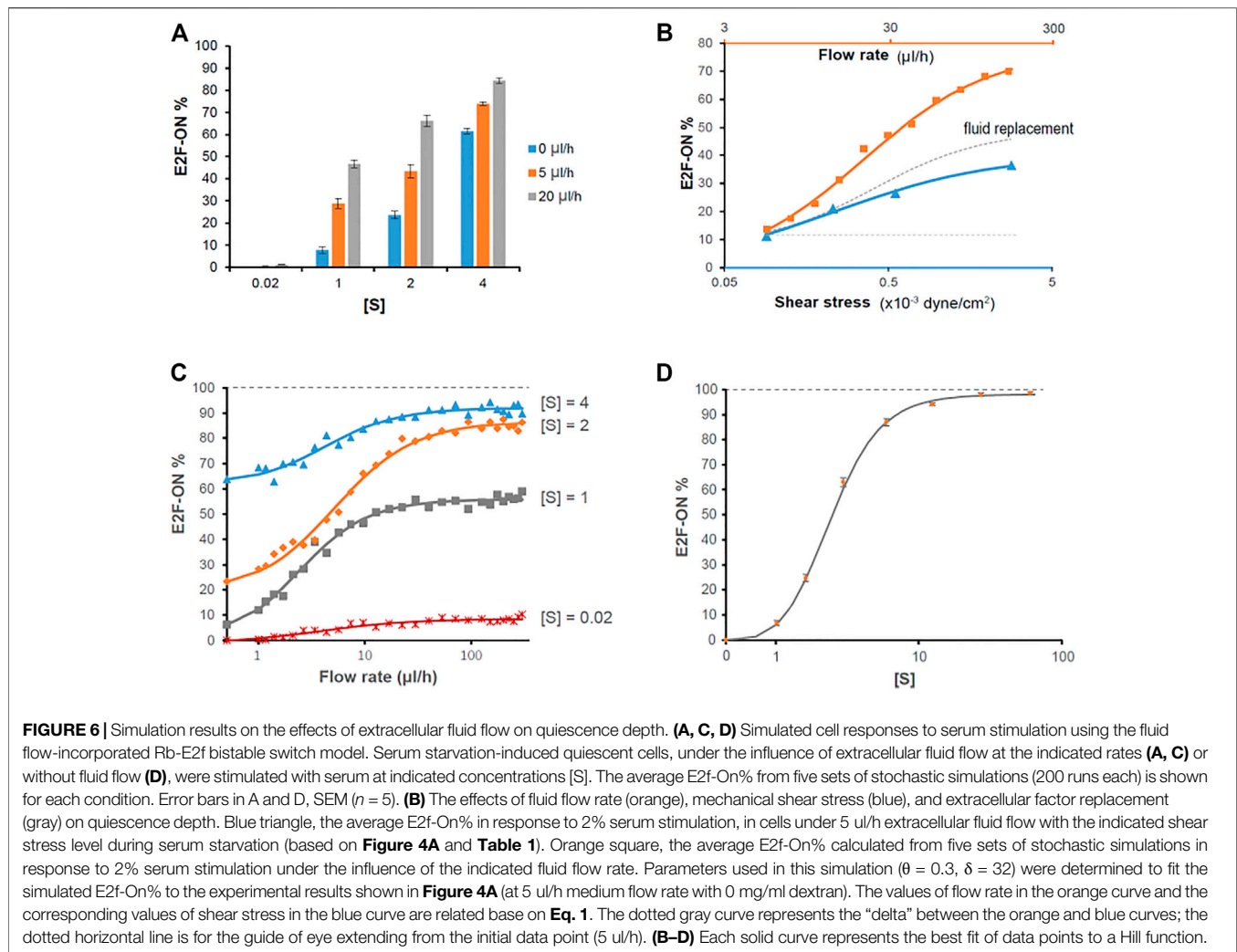
network switch that converts graded and transient serum growth signals into an all-or-none transition from quiescence to proliferation (Yao et al., 2008; Yao et al., 2011). Specifically, the minimum serum concentration required to activate this Rb-E2f bistable switch (the E2f-activation threshold for short) determines quiescence depth (Yao, 2014; Kwon et al., 2017). The experimental results in this study suggested that extracellular fluid flow generates or changes physical (mechanical shear stress) and biochemical (extracellular substances) cues that drive cells to shallow quiescence. We hypothesized that these flow-associated cues boost the cellular responses to serum growth signals and thereby reduce the serum level required to activate the Rb-E2f bistable switch, which results in shallow quiescence.

Accordingly, our previously established mathematical model of the Rb-E2f bistable switch (Yao et al., 2008) was extended, incorporating the extracellular fluid flow effects (FR) into the serum signal terms in the governing ordinary differential equations (ODEs) (**Supplementary Table S1**). The augmented model was utilized to simulate the responses (E2f-On or -Off) of cells to serum stimulation under the influence of extracellular fluid flow varying in rate. The simulations were carried out following the chemical Langevin formulation of the ODE

framework, which considered both intrinsic and extrinsic noise in the system (see Methods for detail), and the results are shown in **Figure 6**.

A direct comparison between **Figure 3B** and **Figure 6A** demonstrates that the simulation results, based on the fluid flow-incorporated Rb-E2f bistable switch model, are qualitatively and quantitatively in good agreement with the experimental measurements. This finding supports our hypothesis regarding how extracellular fluid flow may sensitize cells to serum growth signals and activate the Rb-E2f bistable switch, and thus, reduces quiescence depth. Simulation results further show that the effect of extracellular fluid flow is more pronounced than that of mechanical shear stress alone in promoting quiescence exit (E2f-On%, **Figure 6B**). The "delta" between the two curves (orange minus blue) presumably reflects the effect of extracellular factor replacement in reducing quiescence depth (dotted grey curve, **Figure 6B**); this effect also increases with a higher flow rate (thus, an increasing pace of fluid replacement). Although how shear stress and extracellular factor replacement promote quiescence exit is unknown, taking a simple assumption that shear stress and extracellular factor replacement alone effectively corresponds to a portion (0.75

FIGURE 6 | Simulation results on the effects of extracellular fluid flow on quiescence depth. **(A, C, D)** Simulated cell responses to serum stimulation using the fluid flow-incorporated Rb-E2f bistable switch model. Serum starvation-induced quiescent cells, under the influence of extracellular fluid flow at the indicated rates **(A, C)** or without fluid flow **(D)**, were stimulated with serum at indicated concentrations [S]. The average E2f-On% from five sets of stochastic simulations (200 runs each) is shown for each condition. Error bars in A and D, SEM ($n = 5$). **(B)** The effects of fluid flow rate (orange), mechanical shear stress (blue), and extracellular factor replacement (gray) on quiescence depth. Blue triangle, the average E2f-On% in response to 2% serum stimulation, in cells under 5 ul/h extracellular fluid flow with the indicated shear stress level during serum starvation (based on **Figure 4A** and **Table 1**). Orange square, the average E2f-On% calculated from five sets of stochastic simulations in response to 2% serum stimulation under the influence of the indicated fluid flow rate. Parameters used in this simulation ($\theta = 0.3$, $\delta = 32$) were determined to fit the simulated E2f-On% to the experimental results shown in **Figure 4A** (at 5 ul/h medium flow rate with 0 mg/ml dextran). The values of flow rate in the orange curve and the corresponding values of shear stress in the blue curve are related base on **Eq. 1**. The dotted gray curve represents the "delta" between the orange and blue curves; the dotted horizontal line is for the guide of eye extending from the initial data point (5 ul/h). **(B–D)** Each solid curve represents the best fit of data points to a Hill function.

and 0.85, respectively) of the extracellular fluid flow term FR in the model (**Supplementary Table S1**), the simulation results are reasonably (although not perfectly) consistent with the experimental observations (regarding the shear stress effects, **Supplementary Figure S3**). Together, our modeling and experimental results suggest that the flow-induced shear stress (physical cue) and replacement of extracellular factors (biochemical cues) contribute agnostically to the effect of extracellular fluid flow in promoting quiescence exit by lowering the activation threshold of the Rb-E2f bistable switch.

The good agreement between simulations and experiments motivated the application of the model for predicting the cell responses to higher fluid flow rates above 20 ul/h, under which cells started to partially detach from the microchannel bottom surface and hence excluded from the current experimental study. The simulation results show that the additive effect of extracellular fluid flow to a given serum signal on quiescence exit (E2f-On%) can be well fitted with a Hill function (**Figure 6C**). Namely, E2f-On% increases monotonically with increasing flow rate but is asymptotically bound by a serum concentration-dependent level. By contrast, with sufficiently high serum concentration, the entire cell population can exit quiescence (i.e., E2f-On% approaches 100%) in our model even without extracellular fluid flow (**Figure 6D**). This latter result is consistent with what we experimentally observed previously in REF/E23 cells under static medium (Yao et al., 2008; Kwon et al., 2017; Fujimaki et al., 2019). Therefore, it appears that extracellular fluid flow facilitates quiescence exit by reducing the E2f-activation serum threshold, but unlikely to fully replace the role of serum growth factors in this process.

DISCUSSION

Quiescence is a reversible cellular dormancy state that can persist over prolonged periods of time. The on-demand reactivation of quiescent cells to divide serves as the basis for tissue homeostasis and repair (Coller et al., 2006; Wilson et al., 2008; Cheung and Rando, 2013). Thus far, characteristics of cellular quiescence have been mostly

studied and discovered in conventional static-medium cell cultures, including the basic approaches applied to induce quiescence entry (e.g., serum deprivation, contact inhibition, and loss of adhesion) and exit (by reverting the aforementioned inducing signals). The microenvironment experienced by cultured cells under static medium, however, is different from that experienced by tissue cells *in vivo* where they are exposed to continuous interstitial fluid flows. The interstitial flow exerts hydrodynamic shear stress on cells due to fluid flow viscosity and shear strain rate; the flow also carries fresh nutrients along with dissolved compounds and removes local substances secreted by cells (Jain, 1987; Wiig, 1990; Wang and Tarbell, 1995; Ng and Swartz, 2003; Swartz and Fleury, 2007; Shi and Tarbell, 2011; Freund et al., 2012; Galie et al., 2012). As such, extracellular fluid flow is known to play a critical role in repairing and remolding tissues, such as the vascular, lung, and bone (Hillsley and Frangos, 1994; Liu et al., 1999; Louis et al., 2006; Rensen et al., 2007), through affecting cell morphology, adhesion, motility, metabolism, and differentiation (Yamamoto et al., 2005; Lutolf et al., 2009; Toh and Voldman, 2011; Hyler et al., 2018; Chen et al., 2019). However, whether and how extracellular fluid flow affects cellular quiescence remains unclear.

In this study, a microfluidic platform is designed to mimic the physiologically relevant interstitial fluid flow with varying rates (**Figure 1**) and investigate the flow effects on cellular quiescence. Experimental parameters, including flow rate, fluid viscosity, and flow volume, were varied to test the effects of flow rate, shear stress, and extracellular factor replacement on cellular quiescence depth.

Our results show that, first, several quiescence characteristics identified previously under static medium are also present under continuous fluid flow, including the serum signal-dependant quiescence entry and exit and the time-dependant quiescence deepening (**Figure 2**). Second, extracellular fluid flow sensitizes cells to serum growth signals and thus leads to shallow quiescence. Particularly, increasing the fluid flow rate reduces the serum level needed for quiescence exit and cell cycle reentry. This result is likely due to the extracellular fluid flow lowering the activation threshold of the Rb-E2f bistable switch that controls the quiescence-to-proliferation transition (Yao et al., 2008; Kwon et al., 2017), as suggested by our model simulations (**Figure 6**). A higher fluid flow rate entails higher mechanical shear stress and a faster pace of extracellular factor replacement. These physical and biochemical cues are able to drive cells into shallow quiescence when present either together (**Figure 3**) or separately (**Figures 4, 5**). As a result, exposed to a faster extracellular fluid flow, cells become more sensitive to serum growth signals and more likely to reenter the cell cycle.

Several questions are left unanswered in our study. First, the molecular mechanisms are to be identified by which flow-induced shear stress and extracellular factor replacement lower the activation threshold of the Rb-E2f bistable switch. Interestingly, increasing medium viscosity (by a higher dextran concentration) promotes quiescence exit under a medium flow (**Figure 4**), but it inhibits quiescence exit in static medium (**Supplementary Figure S2**). This result may be associated with medium viscosity-induced changes in certain lipoprotein synthesis (Yedgar et al., 1982), cytoskeleton and cell morphology (Khorshid, 2005), cell attachment and inflammation (Rouleau et al., 2010), or other cellular activities that inhibit quiescence exit in static medium. These changes, if also present under continuous medium flow, appear to be surpassed by the effects of shear stress that promote quiescence exit. The exact mechanism needs to be investigated in future studies. Additionally, quiescent cells cultured in the microfluidic device appear to be generally deeper in quiescence than those cultured in well plates under otherwise the same conditions (e.g., comparing the E2f-On% upon 2% serum stimulation in microdevice (**Figure 3**) and that in the comparable condition in well plate (**Supplementary Figure S2**), both being in static medium, 0 μl/h, and without added dextran). We speculate this difference may be due to the different surfaces that cells were attached to (glass in the microchannel *versus* plastic in the well plate), or different medium height (<0.5 mm in the microchannel *versus* 3–4 mm in the well plate) that could result in different nutrient/factor availability, gas/heat exchange etc., or both. The exact mechanism needs to be further investigated. Nevertheless, the current study demonstrated, for the first time to our best knowledge, the direct effects of extracellular fluid flow and its corresponding components (shear stress and extracellular factor replacement) on cell quiescence depth.

Individual quiescent cells *in vivo*, including stem and progenitor cells in their tissue niches, experience interstitial fluid flows with varying rates and viscosities depending on local tissue structures and distances from nearby blood vessels. The flow-driven heterogeneity in cellular quiescence depth, as demonstrated in this study, may shed light on the heterogeneous responses of quiescent cells in tissue repair and regeneration in different physiological contexts of living tissues.

DATA AVAILABILITY STATEMENT

The original contributions presented in the study are included in the article/**Supplementary Material**, further inquiries can be directed to the corresponding authors.

AUTHOR CONTRIBUTIONS

BL, LJ, JX, YZ, and GY designed research; BL performed experiments; XW performed mathematical modeling and simulation; LJ designed, fabricated, and configured the microfluidic system; BL, LJ, and GY analyzed data; BL, YZ, LJ, and GY wrote the paper.

FUNDING

ACKNOWLEDGMENTS

SUPPLEMENTARY MATERIAL

The Supplementary Material for this article can be found online at: https://www.frontiersin.org/articles/10.3389/fcell.2022.792719/full#supplementary-material

Supplementary Figure S1 | Experimental system configuration and validation. (A) Cell morphology under varying medium flow rates. REF/E23 cells seeded in microfluidic devices were induced to and maintained in quiescence by culturing them in serum-starvation medium for 4 days under the indicated flow rates, then either remained in quiescence (0.02% serum) or stimulated with serum at the indicated concentrations (1–4%) for 26 hours. Phase-contrast images were taken with a 20x objective lens. (B, C) E2f-GFP and EdU-incorporation readouts of cellular quiescence and cell cycle reentry. REF/E23 cells were induced to quiescence as in (A) under a medium flow rate of 5 ul/h (B) or 20 ul/h (C), and then stimulated with serum at the indicated concentrations. Cells were harvested after 26 and 30 hours of simulation, respectively, for E2f-GFP and EdU assays. (Left) Numbers in red indicate the

average E2f-On% or EdU+% as indicated from duplicate samples (black and grey histograms). (Right) Statistic bar chart of E2f-On% and EdU+% from the left-panel histograms. Error bars, SEM (n = 2), * p < 0.05, ** p < 0.01, *** p < 0.001. (D) Dot plots of Fig 3A. Y-axis, forward-scatter; x-axis, E2f-GFP.

Supplementary Figure S2 | The effect of varying dextran concentrations on quiescence depth in static culture. REF/E23 cells were induced to and maintained in quiescence by culturing them in static serum-starvation medium (in well plate) for 4 days with dextran at the indicated concentrations. Cells were subsequently stimulated with serum at the indicated concentrations for 26 hours, and the E2f-On% were assayed. (A) E2f-GFP histograms with red numbers indicating the average E2f-On% from duplicate samples (black and grey). (B) Statistic bar chart of the E2f-On% in cell populations (from A) as a function of dextran concentration (in serum-starvation) and serum concentration (in serum-stimulation). Bar graphs showing the E2f-On% from the left panels. Error bars, SEM (n = 2), * p < 0.05, ** p < 0.01.

Supplementary Figure S3 | Simulation results on the effects of shear stress and extracellular factor replacement on quiescence depth. Simulations of fluid flow rate effects (orange) are the same as in **Figure 6B**. Simulations of the effects of shear stress (red) and extracellular factor replacement (purple) were performed in the same way as the simulations of fluid flow rate effects (orange), except that the FR term in **Supplementary Table S1** was multiplied by 0.75 and 0.85, respectively. Blue triangle, the average E2f-On% in response to 2% serum stimulation, in cells under 5 ul/h extracellular fluid flow with the indicated shear stress level during serum starvation (as in **Figure 6B**, based on **Figure 4A** and **Table 1**). Each solid curve represents the best fit of simulation data points to a Hill function.

REFERENCES

Augenlicht, L., and Baserga, R. (1974). Changes in the G0 State of WI-38 Fibroblasts at Different Times after confluence. *Exp. Cel Res.* 89, 255–262. doi:10.1016/0014-4827(74)90789-7

Bucher, N. L. R. (1963). "Regeneration of Mammalian Liver," in *International Review of Cytology*. Editors G.H. Bourne and J.F. Danielli (New York: Academic Press), 245–300. doi:10.1016/s0074-7696(08)61119-5

Carrasco, F., Chornet, E., Overend, R. P., and Costa, J. (1989). A Generalized Correlation for the Viscosity of Dextrans in Aqueous Solutions as a Function of Temperature, Concentration, and Molecular Weight at Low Shear Rates. *J. Appl. Polym. Sci.* 37, 2087–2098. doi:10.1002/app.1989.070370801

Chen, H., Yu, Z., Bai, S., Lu, H., Xu, D., Chen, C., et al. (2019). Microfluidic Models of Physiological or Pathological Flow Shear Stress for Cell Biology, Disease Modeling and Drug Development. *Trac Trends Anal. Chem.* 117, 186–199. doi:10.1016/j.trac.2019.06.023

Cheung, T. H., and Rando, T. A. (2013). Molecular Regulation of Stem Cell Quiescence. *Nat. Rev. Mol. Cel Biol* 14, 329–340. doi:10.1038/nrm3591

Coller, H. A., Sang, L., and Roberts, J. M. (2006). A New Description of Cellular Quiescence. *Plos Biol.* 4, e83. doi:10.1371/journal.pbio.0040083

Freund, J. B., Goetz, J. G., Hill, K. L., and Vermot, J. (2012). Fluid Flows and Forces in Development: Functions, Features and Biophysical Principles. *Development* 139, 1229–1245. doi:10.1242/dev.073593

Fujimaki, K., Li, R., Chen, H., Della Croce, K., Zhang, H. H., Xing, J., et al. (2019). Graded Regulation of Cellular Quiescence Depth between Proliferation and Senescence by a Lysosomal Dimmer Switch. *Proc. Natl. Acad. Sci. USA* 116, 22624–22634. doi:10.1073/pnas.1915905116

Fujimaki, K., and Yao, G. (2020). Cell Dormancy Plasticity: Quiescence Deepens into Senescence through a Dimmer Switch. *Physiol. Genomics* 52, 558–562. doi:10.1152/physiolgenomics.00068.2020

Galie, P. A., Russell, M. W., Westfall, M. V., and Stegemann, J. P. (2012). Interstitial Fluid Flow and Cyclic Strain Differentially Regulate Cardiac Fibroblast Activation via AT1R and TGF-B1. *Exp. Cel Res.* 318, 75–84. doi:10.1016/j.yexcr.2011.10.008

Gillespie, D. T. (2000). The Chemical Langevin Equation. *J. Chem. Phys.* 113, 297–306. doi:10.1063/1.481811

Hillsley, M. V., and Frangos, J. A. (1994). Review: Bone Tissue Engineering: The Role of Interstitial Fluid Flow. *Biotechnol. Bioeng.* 43, 573–581. doi:10.1002/bit.260430706

Hyler, A. R., Baudoin, N. C., Brown, M. S., Stremler, M. A., Cimini, D., Davalos, R. V., et al. (2018). Fluid Shear Stress Impacts Ovarian Cancer Cell Viability, Subcellular Organization, and Promotes Genomic Instability. *PLoS One* 13, e0194170. doi:10.1371/journal.pone.0194170

Jain, R. K. (1987). Transport of Molecules in the Tumor Interstitium: A Review. *Cancer Res.* 47, 3039–3051.

Khorshid, F. A. (2005). The Effect of the Medium Viscosity on the Cells Morphology in Reaction of Cells to Topography—I. *Proc. 2nd Saudi Sci. Conl, Fac. Sci..* KAU; 15–17 March 2004, Part I, 67–98.

Kwon, J. S., Everetts, N. J., Wang, X., Wang, W., Della Croce, K., Xing, J., et al. (2017). Controlling Depth of Cellular Quiescence by an Rb-E2f Network Switch. *Cel Rep.* 20, 3223–3235. doi:10.1016/j.celrep.2017.09.007

Lee, T. J., Yao, G., Bennett, D. C., Nevins, J. R., and You, L. (2010). Stochastic E2F Activation and Reconciliation of Phenomenological Cell-Cycle Models. *Plos Biol.* 8, e1000488. doi:10.1371/journal.pbio.1000488

Li, L., and Clevers, H. (2010). Coexistence of Quiescent and Active Adult Stem Cells in Mammals. *Science* 327, 542–545. doi:10.1126/science.1180794

Liu, M., Tanswell, A. K., and Post, M. (1999). Mechanical Force-Induced Signal Transduction in Lung Cells. *Am. J. Physiology-Lung Cell Mol. Physiol.* 277, L667–L683. doi:10.1152/ajplung.1999.277.4.L667

Llorens-Bobadilla, E., Zhao, S., Baser, A., Saiz-Castro, G., Zwadlo, K., and Martin-Villalba, A. (2015). Single-Cell Transcriptomics Reveals a Population of Dormant Neural Stem Cells that Become Activated upon Brain Injury. *Cell Stem Cell* 17, 329–340. doi:10.1016/j.stem.2015.07.002

Louis, H., Lacolley, P., Kakou, A., Cattan, V., Daret, D., Safar, M., et al. (2006). Early Activation of Internal Medial Smooth Muscle Cells in the Rabbit Aorta after Mechanical Injury: Relationship with Intimal Thickening and Pharmacological Applications. *Clin. Exp. Pharmacol. Physiol.* 33, 131–138. doi:10.1111/j.1440-1681.2006.04339.x

Lutolf, M. P., Gilbert, P. M., and Blau, H. M. (2009). Designing Materials to Direct Stem-Cell Fate. *Nature* 462, 433–441. doi:10.1038/nature08602

Ng, C. P., and Swartz, M. A. (2003). Fibroblast Alignment under Interstitial Fluid Flow Using a Novel 3-D Tissue Culture Model. *Am. J. Physiology-Heart Circulatory Physiol.* 284, H1771–H1777. doi:10.1152/ajpheart.01008.2002

Orford, K. W., and Scadden, D. T. (2008). Deconstructing Stem Cell Self-Renewal: Genetic Insights into Cell-Cycle Regulation. *Nat. Rev. Genet.* 9, 115–128. doi:10.1038/nrg2269

Owen, T. A., Soprano, D. R., and Soprano, K. J. (1989). Analysis of the Growth Factor Requirements for Stimulation of WI-38 Cells after Extended Periods of Density-dependent Growth Arrest. *J. Cel. Physiol.* 139, 424–431. doi:10.1002/jcp.1041390227

Polacheck, W. J., Charest, J. L., and Kamm, R. D. (2011). Interstitial Flow Influences Direction of Tumor Cell Migration through Competing Mechanisms. *Proc. Natl. Acad. Sci.* 108, 11115–11120. doi:10.1073/pnas.1103581108

Rensen, S. S. M., Doevendans, P. A. F. M., and van Eys, G. J. J. M. (2007). Regulation and Characteristics of Vascular Smooth Muscle Cell Phenotypic Diversity. *Nhjl* 15, 100–108. doi:10.1007/BF03085963

Rodgers, J. T., King, K. Y., Brett, J. O., Cromie, M. J., Charville, G. W., Maguire, K. K., et al. (2014). mTORC1 Controls the Adaptive Transition of Quiescent Stem Cells from G0 to GAlert. *Nature* 510, 393–396. doi:10.1038/nature13255

Rouleau, L., Rossi, J., and Leask, R. L. (2010). Concentration and Time Effects of Dextran Exposure on Endothelial Cell Viability, Attachment, and Inflammatory Marker Expression *In Vitro. Ann. Biomed. Eng.* 38, 1451–1462. doi:10.1007/s10439-010-9934-4

Sang, L., Coller, H. A., and Roberts, J. M. (2008). Control of the Reversibility of Cellular Quiescence by the Transcriptional Repressor HES1. *Science* 321, 1095–1100. doi:10.1126/science.1155998

Shi, Z.-D., and Tarbell, J. M. (2011). Fluid Flow Mechanotransduction in Vascular Smooth Muscle Cells and Fibroblasts. *Ann. Biomed. Eng.* 39, 1608–1619. doi:10.1007/s10439-011-0309-2

Shirure, V. S., Lezia, A., Tao, A., Alonzo, L. F., and George, S. C. (2017). Low Levels of Physiological Interstitial Flow Eliminate Morphogen Gradients and Guide Angiogenesis. *Angiogenesis* 20, 493–504. doi:10.1007/s10456-017-9559-4

Spencer, S. L., Cappell, S. D., Tsai, F.-C., Overton, K. W., Wang, C. L., and Meyer, T. (2013). The Proliferation-Quiescence Decision Is Controlled by a Bifurcation in CDK2 Activity at Mitotic Exit. *Cell* 155, 369–383. doi:10.1016/j.cell.2013.08.062

Swartz, M. A., and Fleury, M. E. (2007). Interstitial Flow and its Effects in Soft Tissues. *Annu. Rev. Biomed. Eng.* 9, 229–256. doi:10.1146/annurev.bioeng.9.060906.151850

Tarbell, J. M., Weinbaum, S., and Kamm, R. D. (2005). Cellular Fluid Mechanics and Mechanotransduction. *Ann. Biomed. Eng.* 33, 1719–1723. doi:10.1007/s10439-005-8775-z

Toh, Y. C., and Voldman, J. (2011). Fluid Shear Stress Primes Mouse Embryonic Stem Cells for Differentiation in a Self-renewing Environment via Heparan Sulfate Proteoglycans Transduction. *FASEB j.* 25, 1208–1217. doi:10.1096/fj.10-168971

Wang, D. M., and Tarbell, J. M. (1995). Modeling Interstitial Flow in an Artery Wall Allows Estimation of Wall Shear Stress on Smooth Muscle Cells. *J. Biomechanical Eng.* 117, 358–363. doi:10.1115/1.2794192

Wang, X., Fujimaki, K., Mitchell, G. C., Kwon, J. S., Della Croce, K., Langsdorf, C., et al. (2017). Exit from Quiescence Displays a Memory of Cell Growth and Division. *Nat. Commun.* 8, 321. doi:10.1038/s41467-017-00367-0

Wiig, H. (1990). Evaluation of Methodologies for Measurement of Interstitial Fluid Pressure (Pi): Physiological Implications of Recent Pi Data. *Crit. Rev. Biomed. Eng.* 18, 27–54.

Wilson, A., Laurenti, E., Oser, G., van der Wath, R. C., Blanco-Bose, W., Jaworski, M., et al. (2008). Hematopoietic Stem Cells Reversibly Switch from Dormancy to Self-Renewal during Homeostasis and Repair. *Cell* 135, 1118–1129. doi:10.1016/j.cell.2008.10.048

Yamamoto, K., Sokabe, T., Watabe, T., Miyazono, K., Yamashita, J. K., Obi, S., et al. (2005). Fluid Shear Stress Induces Differentiation of Flk-1-Positive Embryonic Stem Cells into Vascular Endothelial Cells *In Vitro. Am. J. Physiology-Heart Circulatory Physiol.* 288, H1915–H1924. doi:10.1152/ajpheart.00956.2004

Yao, G., Lee, T. J., Mori, S., Nevins, J. R., and You, L. (2008). A Bistable Rb-E2f Switch Underlies the Restriction point. *Nat. Cel Biol* 10, 476–482. doi:10.1038/ncb1711

Yao, G. (2014). Modelling Mammalian Cellular Quiescence. *Interf. Focus.* 4, 20130074. doi:10.1098/rsfs.2013.0074

Yao, G., Tan, C., West, M., Nevins, J. R., and You, L. (2011). Origin of Bistability Underlying Mammalian Cell Cycle Entry. *Mol. Syst. Biol.* 7, 485. doi:10.1038/msb.2011.19

Yao, W., Li, Y.-b., and Chen, N. (2013). Analytic Solutions of the Interstitial Fluid Flow Models. *J. Hydrodyn* 25, 683–694. doi:10.1016/s1001-6058(13)60413-8

Yedgar, S., Weinstein, D. B., Patsch, W., Schonfeld, G., Casanada, F. E., and Steinberg, D. (1982). Viscosity of Culture Medium as a Regulator of Synthesis and Secretion of Very Low Density Lipoproteins by Cultured Hepatocytes. *J. Biol. Chem.* 257, 2188–2192. doi:10.1016/s0021-9258(18)34904-4